Procedia Manufacturing

Volume 5, 2016, Pages 558–567

44th Proceedings of the North American Manufacturing Research Institution of SME http://www.sme.org/namrc

Numerical Investigation of Transient Temperature and Residual Stresses in Thin Dissimilar Aluminium Alloy Plates

Tapas Bajpei, H. Chelladurai and Mohd. Zahid Ansari*

PDPM Indian Institute of Information Technology, Design and Manufacturing, Dumna Airport Road, Khamaria, Jabalpur-482005, Madhya Pradesh, India

tapasbajpei03@gmail.com, chella@iiitdmj.ac.in, zahid@iiitdmj.ac.in

Abstract

The purpose of the present investigation is to assess transient temperature and residual stresses in Gas Metal Arc Welding (GMAW) of dissimilar aluminium alloys (AA). A moving heat source model based on Goldak's double – ellipsoid heat flux distribution is utilised in finite element simulation of welding process. To solve the three dimensional thermal and mechanical equations, ANSYS Workbench software was used. Element death and birth code was written for modelling the amount of material added during the analysis. Effects of conduction, convection and radiation were considered in transient thermal analysis. Temperature dependent properties as thermal conductivity, heat capacity, yield stress, elastic modulus and thermal expansion were employed in the welding simulations. Based on the results, it was found that lower temperature and higher residual stresses were generated in AA 6061-T6 plate as compared to AA 5052-H32 plate.

Keywords: Gas metal arc welding (GMAW), finite Element analysis, residual stresses, ANSYS Workbench

1 Introduction

Gas Metal Arc Welding (GMAW) is popularly used for joining aluminium alloys. The process offers high welding speed with versatility and provides high-quality welding joints. Despite of many advantages, residual stresses are inevitable in GMAW weldments. These stresses are generated due to non uniform thermal expansion and contraction of material associated with localised transient heating and non-linear temperature profiles produced in the structure during welding. Residual stresses are undesirable in welded components as they results in fatigue failure, stress corrosion cracking and impair the buckling strength of components. Detrimental effects of residual stresses due to non-

* Corresponding author.

 Selection and peer-review under responsibility of the Scientific Programme Committee of NAMRI/SME

doi:10.1016/j.promfg.2016.08.046

uniform heating is more pronounced in thin sheets as they offer less stiffness to resist the contraction forces generated during the welding process.

Dissimilar joints are prepared between two materials having distinct mechanical and chemical properties. During fusion welding of dissimilar joints, mingling of filler material and base metal occurs. The resulting material produced around the weld zone due to mixing process has different mechanical properties from the parent material and affects temperature and residual stress distribution. Thus, it is necessary to understand their distribution in dissimilar materials. Atabaki et al. [2014] used a three-dimensional finite element model in order to comprehend temperature and heat distribution in aluminium alloy 5000 and 6000 series joined by hybrid laser arc welding. Kumarsen et al. [2011] predicted the stress distribution in aluminium alloy plates during TIG welding. They applied ANSYS "Element death and birth" codes for simulating material, added during TIG welding process. Mousavi and Miresmaeili [2008] utilized X-ray diffraction technique for predicting the effect of grooves configurations on residual stress distribution during TIG welding process. Ranjbarnodeh et al. [2011] developed a thermo-mechanical model in order to study the effect welding parameters on the distribution of residual stresses during TIG welding of low carbon and ferritic stainless steel. They also investigated the effect of length of specimen and welding speed on residual stress distribution. They found that with increase in welding current and length of specimen residual stress in weldment decreases. Riahi and Nazari [2011] investigated transient temperature field and residual stress distribution in AA 6061-T6 during friction stir welding process. They reported that higher temperature gradient exists in region under the shoulder of the rotating tool. Also, with increase in tool speed, higher value of longitudinal stress was observed in the weld plate. Ranjabarnodeh et al. [2011] developed two- dimensional thermo-elastic-plastic model to predict the residual stress in TIG welded plain carbon steel CK4 and ferritic stainless steel AISI409. Zhu and Chao [2002] carried out 3D finite element analysis to ascertain the residual stresses in thick plates of AA 5052-H32. They considered elastic-plastic material properties at different temperature for computational simulation.

In the present study, a thermal-mechanical model is developed in order to calculate temperature distribution and residual stresses in thin dissimilar square butt joint of AA 5052-H32 and AA 6061-T6 plates. To solve the governing heat transfer and elastic-plastic equations a sequentially coupled transient thermal-static structural system is employed in commercial finite element analysis software ANSYS workbench 15.0. Temperature dependent material properties, thermal and mechanical boundary conditions, latent heat effect as well as Goldak's volumetric heat source model are considered. Element death and birth procedure is adopted during simulation in order to activate and deactivate the elements describing the filler material.

2 Finite Element Analysis

To develop a model for the GMAW process, different process parameters such as the number of finite element solution steps and sub steps, the weld speed and deposition of filler, and material nonlinearities have been considered. Following assumptions with regard to the finite element thermal-structural analysis are considered: (1) convection effects due to argon and air and radiation phenomenon have been considered, (2) finite element death and birth procedure is used for simulating the filler metal deposition during welding process, and (3) temperature dependent properties have been considered for analysis. For performing the simulation two analysis systems (transient thermal- static structural) were coupled together in order to simulate the temperature and residual stress fields during GMA welding. During initial phase of simulation, a non-linear transient thermal analysis was carried out to find out thermal distribution on weld plates during the welding and cooling processes. Subsequently, the obtained nodal temperatures from thermal analysis were applied as 'body force' loads in structural analysis.

Finite element software ANSYS Workbench 15.0 was used to investigate the welding residual stresses. In the present investigation, two different types of aluminium alloys, AA 5052-H32 and AA 6061-T6 was used. Plates of dimensions 200 × 150 × 3 mm^3 were used in the analysis. Fine meshing was provided near to the weld zone and gradually coarse mesh for distant zones. This was done because higher temperature and stress gradients exist near the weld line and to improve the accuracy of the model. Figure 1 shows 3D FEM model used in thermal and structural analysis. Three dimensional SOLID90 elements were used for the thermal analysis. For structural analysis SOLID186 elements were used. Total 17849 elements were used to simulate both thermal and structural analysis.

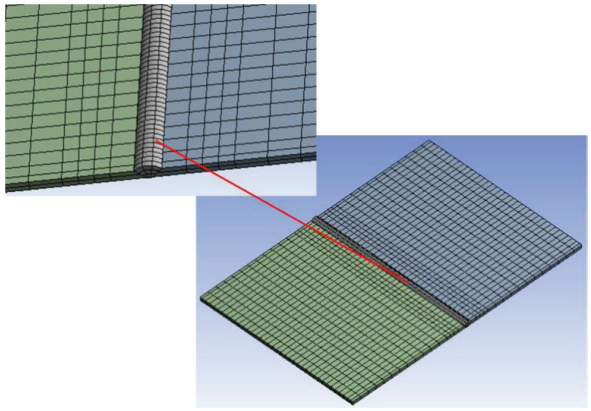

Figure 1: Finite element mesh of the butt weld.

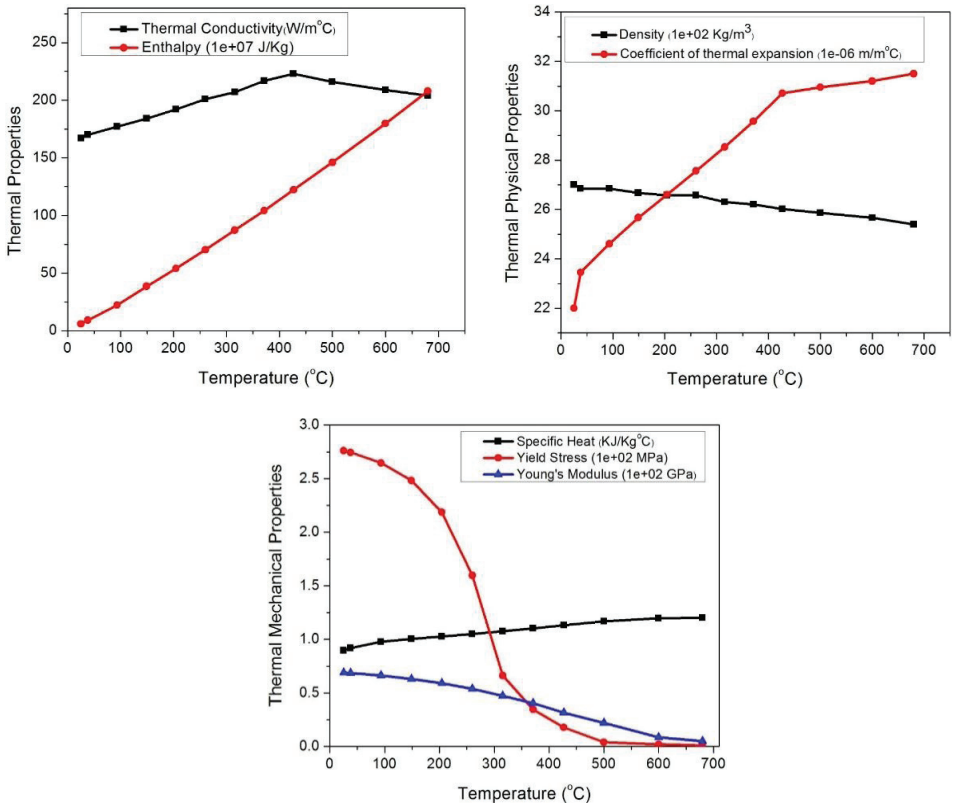

Figure 2: Variation of thermal and mechanical properties with temperature in AA 6061-T6.

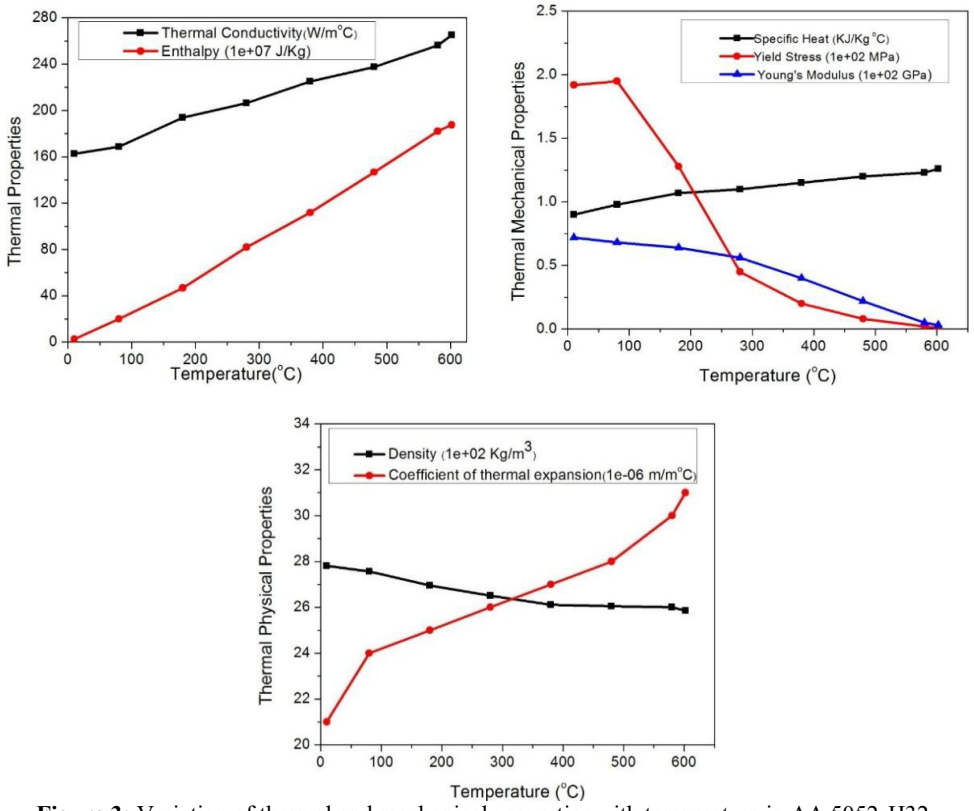

Figure 3: Variation of thermal and mechanical properties with temperature in AA 5052-H32.

Temperature dependent thermal and mechanical properties of AA 5052- H32 and 6061-T6 were used in order to predict transient temperature fields, Zhu and Chao (2002), Riahi and Nazari (2011). Temperature dependent properties of aluminium alloys (6061-T6 and 5052-H32) used in simulation are presented in figure 2 and figure 3. Poisson's ratio (v) value was assumed as 0.34. The tangent modulus was considered to be 0.5% of the Young's modulus at the corresponding temperature, Bhatti et.al (2015). The filler material used in the investigation is ER5356. Its chemical composition (wt %) is Al =94.38, Mg = 4.5, Cr = 0.05, Mn = 0.05, Si = 0.25, Zn = 0.1. Its mechanical properties as density = 2657 kg/m^3, yield strength (with base alloy 6061-T6) = 210 MPa, tensile strength (with base alloy 6061-T6) = 2105 MPa, percentage elongation (with base alloy 6061-T6) = 11%. Since the variation in the mechanical and thermal properties of filler material (ER 5356) and AA 5052-H32 are similar, properties of AA 5052-H32 is used for the filler material, ESAB ER5356 (2016).

2.1 Thermal Analysis

In order to determine transient temperature fields in a three dimensional body during welding process the following partial differential equation can be used, Incropera et.al. (2007):

$$\frac{\partial}{\partial x}\left(k_x \frac{\partial T}{\partial x}\right) + \frac{\partial}{\partial y}\left(k_y \frac{\partial T}{\partial y}\right)) + \frac{\partial}{\partial z}\left(k_z \frac{\partial T}{\partial z}\right) + \dot{q_g} = \rho c_p \frac{\partial T}{\partial \tau} \tag{1}$$

where T (x, y, z, τ) is the temperature, and x, y, z represents the welding directions in longitudinal, transverse and thickness directions, $\dot{q_g}$ is rate of internal heat generation, τ is time, ρ is the density, c_p is the specific heat, k_x, k_y, k_z are the thermal conductivities in x, y and z directions, respectively. Initial

conditions are defined as $T(x, y, z, 0) = T_0(x, y, z)$. Initial condition used in the mathematical model was: $T_o = 28\ ^oC$.

While applying thermal boundary conditions, heat dissipated due to both convection and radiation was considered. Convective boundary conditions due to flow of air was applied on the horizontal surfaces & vertical edges of the plate. The convection caused by the flow of shielding gas (argon) was employed in the weld zone vicinity on top surface of the plate. Values of convective heat transfer coefficient used for argon and air are 15 W/m^2 ^{o}C and 3.5 W/m^2 ^{o}C, respectively. On substituting the initial condition and thermal boundary conditions, the general solution for Eq. (1) is, Mousavi and Miresmaeilli (2008):

$$k\frac{\partial T}{\partial x}\, l_x + k\frac{\partial T}{\partial y} l_y + k\frac{\partial T}{\partial z} l_z + q_f + h_{conv}\,(T_s - T_0) + \sigma\epsilon(\,T_s^4 - T_0^4) = 0 \tag{2}$$

where, l_x, l_y, and l_z are direction cosines of the outward drawn normal to the boundary, h_{conv} is the heat transfer coefficient, q_f is the boundary heat flux, ϵ is emissivity whose valve considered is 0.03 and σ = 5.67 × 10^{-8} W/m^2 ^{o}C is Stefan- Boltzmann constant.

To include the effect of latent heat due to phase change, the enthalpy was used as $\Delta h^* = \int \rho(T)\, c_p\,(T) dT$. This function was calculated from previous values of density (ρ) and specific heat (c_p) at the same temperature, Capriccioli and Frosi (2009). The integration arbitrary constant was defined equal to the product $\rho c_p T$ at 0 ^{o}C. To calculate the magnitude of enthalpy at the liquidus temperature latent heat value is added at the solidus temperature, Specific heat and density do not differ much in the liquid phase thus they are assumed to be constant. Hence the enthalpy in that range has a constant slope given by the last values defined for c_p and ρ. In the present study, latent heat of fusion of 389 KJ/kg was used for AA 5052-H32 in order to calculate the enthalpy value at liquidus temperature. The mechanical boundary conditions were defined by using fixed supports in order to simulate clamping of aluminium alloy plates. Also displacement boundary conditions were applied in steps on filler material i.e. ($u_x = u_y = u_z = 0$). It is as shown in figure 4.The complete procedure was executed by writing APDL codes in ANSYS Workbench. Element death and birth approach was adopted to simulate the addition of filler material during the welding process. Firstly, the elements representing the filler material in the groove were killed. During the element killing the ANSYS deactivates the elements by multiplying their stiffness with a small factor to neglect their contribution in the analysis. The default value of this factor is 10^{-6}, ANSYS (2013). Further, elements were born in subsequent steps. When the elements were reactivated its stiffness returns to their original values.

For modeling the movement of welding heat source, a 3D heat source model proposed by Goldak was used. The rate of volumetric heat flux distributions of the front and rear quadrants of the moving heat source are expressed as, Goldak et al. (1984, 2005):

$$q_f(x,y,z,t) = \frac{6\sqrt{3} f_f\ Q}{a_f b_f c_f \pi\sqrt{\pi}}\ exp\frac{-3x^2}{a^2}\ exp\frac{-3[y + s*(\tau - t)]^2}{b_f^2}\ exp\frac{-3z^2}{c^2}\ \left[\frac{J}{m^3 s}\right] \tag{3}$$

$$q_r(x,y,z,t) = \frac{6\sqrt{3} f r\ Q}{a_r b_r c_r \pi\sqrt{\pi}}\ exp\frac{-3x^2}{a^2}\ exp\frac{-3[y + s*(\tau - t)]^2}{b_r^2}\ exp\frac{-3z^2}{c^2}\ \left[\frac{J}{m^3 s}\right] \tag{4}$$

where x, y, z are the local coordinates of the ellipsoidal model, τ is lag factor required to describe the location of heat source at time $t = 0$, $\tau = r/s$, s is the welding speed, r = characteristic radius of flux distribution, $Q = \eta VI$ is the electric power of the arc available for melting the joint, V is welding voltage, I is welding current, η is efficiency of the heat source in GMAW process and was assumed as η = 75%, Kou (2003). F_f and F_r are the weighting fractions of the heat distributed in front and rear quadrants respectively. The constants a, b_f, b_r, c, f_f, f_r in Eq. (3) and (4) are heat source parameters

which define weld pool dimensions and thus distribution of heat flux. 'b_f' is the weld length in the front part of the weld and 'a' is also estimated as the half width of the weld pool. 'b_r' denotes the weld length in rear part and 'c' is the weld penetration, Kohandehghan and Serajzadeh (2011). The values of calculated heat source parameters were assumed as a = 5.13 mm, b_f = 5.13 mm, b_r = 5.13 mm, c = 3 mm, f_f = 0.39 and f_r = 1.6 respectively. Initially the location of the heat source was x_i = 0 mm, y_i = 0 mm and z_i = 3 mm.

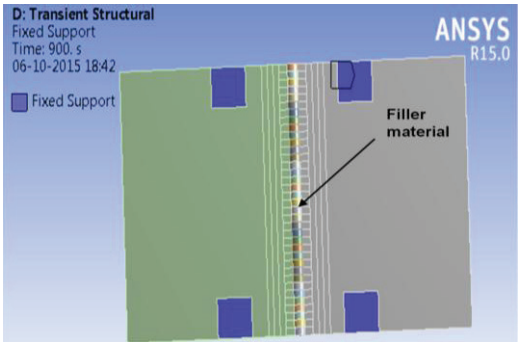

Figure 4: Mechanical boundary conditions.

2.2 Structural Analysis

For calculating the residual stresses during welding process, thermo-elastic-plastic formulations were used. As the material properties depend upon the temperature history, the resulting stresses and strains depend upon the path. They are obtained by applying thermal loads step-by-step during thermal analysis. The resulting stresses and strains were calculated by utilizing incremental stress-strain relationships presented as, Ueda and Nakqacho (1980):

$$\{d\dot{\varepsilon}_{ij}^{nth}\} = [\{d\dot{\varepsilon}_{ij}^{E}\} + \{d\dot{\varepsilon}_{ij}^{P}\} + \{d\dot{\varepsilon}_{ij}^{TH}\}] \quad (5)$$

where, $d\dot{\varepsilon}_{ij}^{E}$ is elastic strain, $d\dot{\varepsilon}_{ij}^{P}$ is plastic strain and $d\dot{\varepsilon}_{ij}^{TH}$ is thermal strain. The movement of welding torch was simulated along the centre line of the weld. Depending on the welding speed total number of 37 solution steps and two sub steps were used to model the moving heat source. In every step one element was added and volumetric heat flux calculated from Equation 3 and 4 was applied on these elements. Finally, last step was performed for 900 seconds in order to execute the cooling cycle of weld plates to the ambient temperature.

3 Results and Discussion

Figure 5 shows the transient temperature distribution in AA plates after 10 seconds. As the heat source advances, the temperature starts reducing due conduction and convection effects. From figure it is observed that extremely high temperature gradient exists at the weld region due to the intense heat energy provided by GMA welding. The temperature distribution in AA weldment is asymmetric because of the different thermo-physical properties of aluminium alloys. Figure 6 illustrates the transient temperatures distribution calculated at x = 7.5 mm, 12.5 mm, 17.5 mm, y = 110 mm, z = 3 mm. From figures, it can be seen that the peak temperature probed in the heat affected zone is 540 ^{o}C in AA 5052-H32 plate and 342 ^{o}C in AA 6061-T6 plate. Less temperature in AA 6061-T6 is due to its higher thermal conductivity as compared to AA 5052-H32.

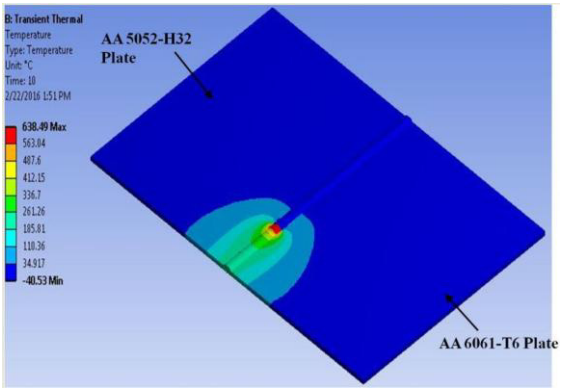

Figure 5: Temperature distribution (after 10 sec.) in aluminium alloy plates during GMA welding process.

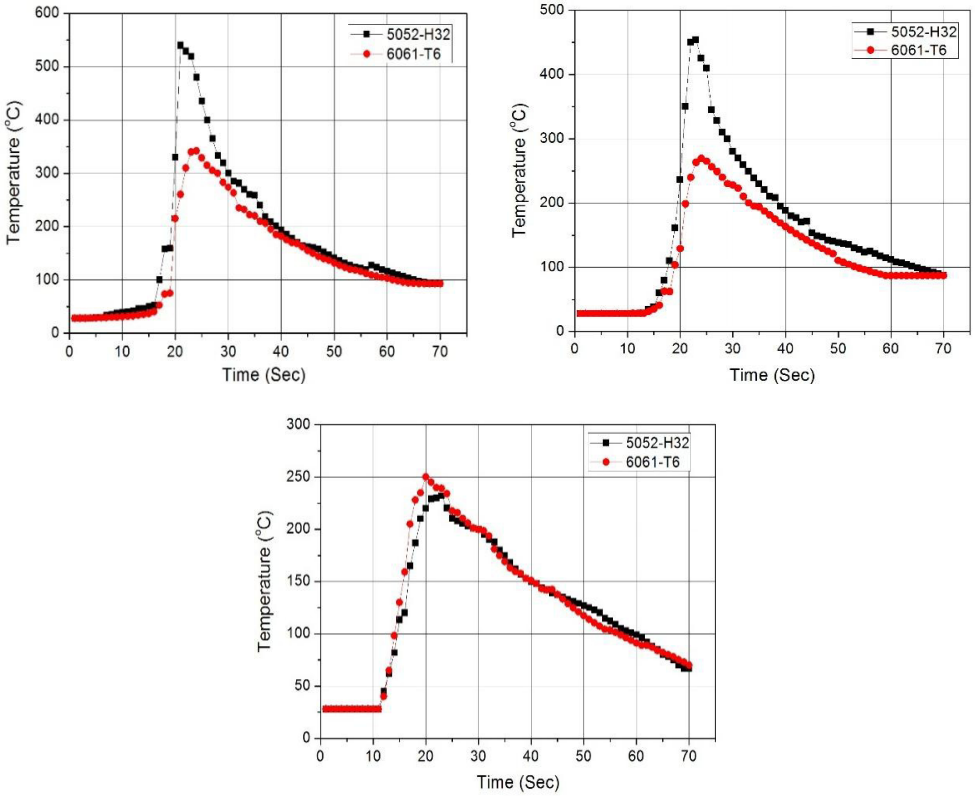

Figure 6: Comparison of experimental and numerical FEM transient temperature results in AA 5052-H32 plates at a distance of 7.5 mm (top-left), 12.5 mm (top-right) and 17.5 mm (bottom) from weld centre.

The corresponding von Mises equivalent stress distribution in aluminium alloy plates during GMA welding process is shown in Figure 7. From figure, it is observed that high residual stresses are developed in weld zone vicinity and heat affected zone (HAZ). The maximum value of equivalent stress is found to be 132 MPa for AA 6061-T6 and 107 MPa for AA 5052-H32. Also, it can be perceived that compressive stress is developed around the clamping zones. This is due to the presence of fixture which restrains the movement of plate. Figure 8 shows the finite element (FE) results for longitudinal and transverse stresses originated during GMAW process. High value of longitudinal

stress of about 292 MPa is observed in AA 6061-T6 plate as compared to AA 5052-H32 plate in which the value of longitudinal stress is found to be about 187 MPa. This is because the yield strength of AA 6061-T6 (276 MPa) is more as compared to the yield strength of AA 5052-H32. Figure 9 illustrates the distribution of transverse and longitudinal stresses measured at different distances on top surface of the weldment. It is observed that compressive transverse stress is developed around the weld zone which is gradually changing its nature to tensile stress when moving away from the weld bead. The possible reason is the contraction of weld metal is prevented by relatively cold parent material.

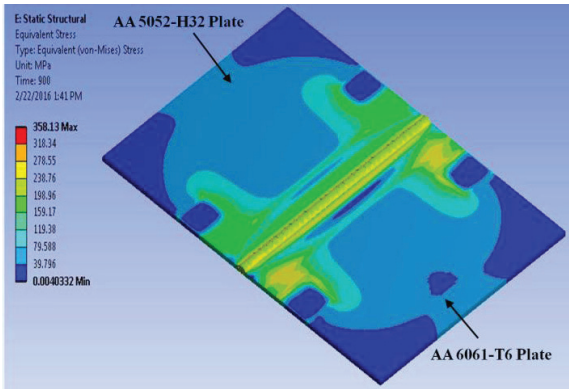

Figure 7: Contour of von Mises equivalent residual stress in GMA welding process.

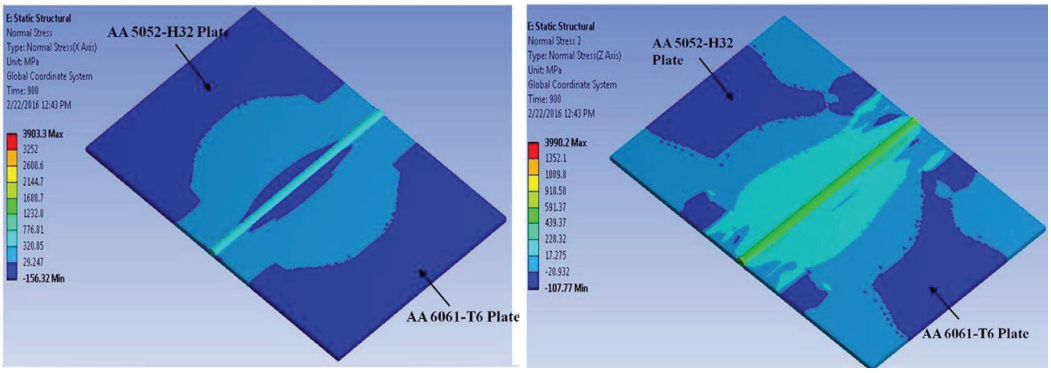

Figure 8: Residual stress distribution in GMAW process in longitudinal (left) and transverse (right) directions.

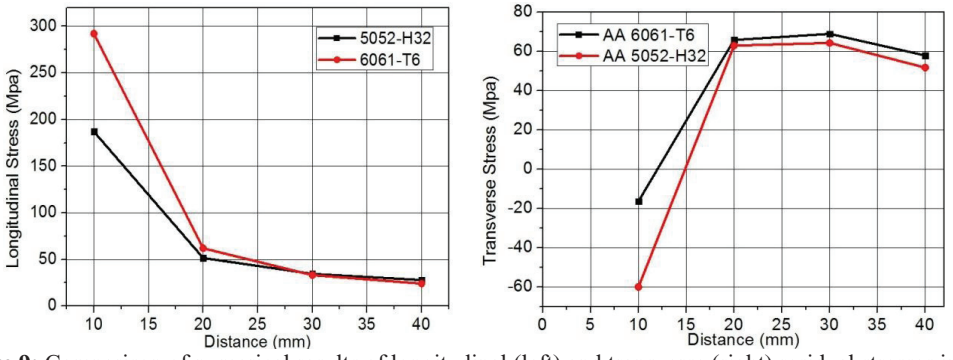

Figure 9: Comparison of numerical results of longitudinal (left) and transverse (right) residual stresses in AA 5052-H32 plate and AA 6061-T6 plate.

4 Conclusions

In the present investigation a 3D non-linear thermal-mechanical finite element model has been developed to predict the temperature and stress fields during GMA welding of AA 5052- H32 and AA 6061-T6. Numerically obtained results show that:

- In dissimilar weldment, high value of residual stresses is found in AA 6061-T6 plate because of its higher yield strength value.
- Low values of temperatures are found in AA 6061-T6 plate because of its higher thermal conductivity as compared to AA 5052-H32 plate.
- The finite element method including death and birth procedure is an effective method to predict residual stresses in the weld zone, HAZ and base material.

Nomenclature

c_p	specific heat (kJ/kg℃)
T_s	temperature of the surface (℃)
T_0	ambient temperature(℃)
$\overline{Nu_l}$	average Nusselt number
$\bar{h}$	average convection heat transfer coefficient (W/m^2 ℃)
k	thermal conductivity (W/m℃)
$q_g^{\cdot}$	rate of internal heat generation (W/m^3)
Ra_L	Rayleigh number
s	welding speed (mm/s)
r	characteristic radius of flux distribution (mm)
h^*	enthalpy (KJ/kg)

Greek letters

ρ	density (Kg/m^3)
ν	Poisson's ratio
$d\dot{\varepsilon}_{ij}^{E}$	elastic strain
$d\dot{\varepsilon}_{ij}^{P}$	plastic strain
$d\dot{\varepsilon}_{ij}^{TH}$	thermal strain
α	coefficient of thermal expansion (10^{-6}/ ℃)

References

ANSYS Mechanical APDL Advanced Analysis Guide/ANSYS help, release 15.0 2013, Canonsburg, USA, 2013.

Atabaki MM, Nikodinovski M, Chenier P, Ma J, Liu W and Kovasevic R. Experimental and numerical investigations of hybrid laser arc welding of aluminium alloys in thick T joint configuration. Optics and Laser Technology 2014; 59:68-92.

Bhatti AA, Barsoum Z, Murakawa H and Barsoum I. Influence of thermo-mechanical material properties of different steel grades on welding residual stresses and angular distortion, Materials and Design 2015; 65:878-889.

ESAB ER5356. E:\NAMRC\NAMRC\ER 5356\ESAB ER5356 _ Welding Consumables _ Products & Solutions.html [retrieved February 29, 2016]

Incropera F, Dewitt D, Bergman T and Lavine A. Fundamentals of Heat and Mass Transfer. 2007:71-72.

Mousavi-Akbari SAA and Miresmaelli R. Experimental and numerical analyses of residual stress distributions in TIG welding process for 304L stainless steel. Journal of Materials Processing Technology 2008; 208:383-394.

Capriccioli A and Frosi P. Multipurpose ANSYS FE procedure for welding process simulation, Fusion Engineering and Designing 2009; 84:546-553.

Goldak J, Chakravarti A and Bibby M. A new finite element model for welding heat sources, Metallurgical Transactions B 15B 1984; 15: 299-305.

Goldak J and Akhlaghi M. Computational Welding Mechanics. 2005; 30-35.

Kohandehghan AR and Serajzadeh S. Arc welding induced residual stress in butt- joints of thin plates under constraints, Journal of Manufacturing Processes 2011; 13:96-103.

Kumaresan D, Asraff A K and Muthukumar R. Numerical investigation on heat transfer and residual stress in butt welded plate, Journal of Pressure Vessel Technology 2011; 133:1-10.

Ranjbarnodeh E, Serajzadeh S, Kokabi AH, Hanke S and Fischer A. Finite element modelling of the effect of heat input on residual stresses in dissimilar joints. International Journal of Advance Manufacturing Technology 2011; 55: 649-656.

Riahi M and Nazari H. Analysis of transient temperature and residual stresses in friction stir welding of aluminium alloy 6061- T6 via numerical simulation. International Journal of Advance Manufacturing Technology 2010; 55:143-152.

Ranjabarnodeh E, Serajzadeh S, Kokabi AH and Fischer A. Effect of welding parameters on residual stresses in dissimilar joints of stainless steel to carbon steel. Journal of Mater Science 2011; 46: 3225-3232.

Ueda Y and Nakqacho K. Theory of thermal elastic-plastic analysis with a more general work hardening rule. Trans JWRI 1984; 9:107-114.

Zhu XK and Chao YJ. Effect of temperature dependent material properties on welding simulation. Computers and Structures 2002; 80:967-976.